Draft version July 9, 2025
Typeset using LaTeX **twocolumn** style in AASTeX7

Spectroscopic Orbits of Subsystems in Multiple Stars. XI

Andrei Tokovinin[1]

[1] *Cerro Tololo Inter-American Observatory, NSF's NOIRLab Casilla 603, La Serena, Chile*

ABSTRACT

Adding to the large radial velocity survey of nearby solar-type stars (summary in Tokovinin, 2023a), spectroscopic orbits are determined for four hierarchical systems: HIP 49442 (inner and outer periods of 164.55 d and 34 yr, respectively), HIP 55691 (2.4 and 415 yr), HIP 61465 (86.8 d), and HIP 78662C (0.82 d). Each system is discussed individually. Seven Gaia orbits of low-mass dwarfs, each with two additional resolved (interferometric and wide) companions, i.e. potential quadruples, are tested by monitoring radial velocities; five orbits are confirmed and two are refuted. Five of these systems are quadruples of 3+1 hierarchy, one is quintuple, and one is triple. Strengths and limitations of the Gaia data on multiple systems and the need of complementary observations are highlighted.

Keywords: Multiple Stars (1081) — Binary Stars (154) — Spectroscopic binary stars (1557) — Visual binary stars (1777)

1. INTRODUCTION

Hierarchical systems of three or more stars are an important constituent of the stellar population. Statistical knowledge of their architecture (distributions of periods, eccentricities, masses, and multual inclinations) is informative both for the star formation theory and for the population synthesis of stellar evolution. Owing to the huge range of periods and separations, coverage of the full parameter space requires combination of several observing techniques, and at present it is still very incomplete. This work contributes spectroscopic orbits of several nearby hierarchies.

The Gaia mission (Gaia Collaboration et al. 2016, 2021a) provides precise astrometry and other information uniformly for the whole sky. Within 100 pc, there are about 8000 pairs of Gaia sources with separations above ∼100 au and indications of an inner subsystem (an elevated reduced unit weight error, RUWE, or multipeak transits) in one or both components (A. Tokovinin 2023a). However, Gaia informs us on the parameters of these subsystems only for a small subset of stars with astrometric or spectroscopic orbits (inner periods below 3 yr). Furthermore, hierarchies with outer separations under 100 au (the most interesting ones) are revealed by Gaia only exceptionally by cross-matching different multiplicity indicators (D. R. Czavalinga et al. 2023; D. Bashi & A. Tokovinin 2024). Parallaxes of many pairs with separations under 1″ are not provided in the Gaia data release 3 (GDR3), and those binaries and hierarchies are missing from the Gaia catalog of nearby stars, GCNS (Gaia Collaboration et al. 2021b). Even within 20 pc, a significant fraction of stars and brown dwarfs lack Gaia astrometry, their multiplicity being one of the culprits (J. D. Kirkpatrick et al. 2024). Therefore, complementary ground-based work on multiplicity is essential in the Gaia era, and this will remain true after the final Gaia data release.

Hierarchical systems are often discovered by variable radial velocity (RV) in resolved ("visual") binary stars. Without follow-up work, however, parameters of inner subsystems remain unknown. A large RV survey of nearby solar-type hierarchies has been conducted to determine these parameters (A. Tokovinin 2023b). It is complemented here by the detailed analysis of four additional hierarchies, overlooked originally. This project, started before Gaia, shows that only a third of spectroscopic orbits appear in the Gaia NSS (nonsingle star catalog, Gaia Collaboration et al. 2023), and not all Gaia spectroscopic orbits are correct (see also D. Bashi et al. 2022; E. Gosset et al. 2025). The reasons are the complexity of the RV signals from hierarchical systems and avoidance of stars with resolved companions in the NSS.

The second part of this paper reports a test of Gaia orbits in a subset of hierarchies within 100 pc observed by speckle interferometry (A. Tokovinin 2023a). Their short Gaia periods do not match the longer periods of the speckle companions, suggesting that these systems are at least quadruple, considering also the distant Gaia

Table 1. Spectroscopic Orbits

HIP/ GKM	System	P (d)	T (JD -2,400,000)	e	ω_A (deg)	K_1 (km s^{-1})	K_2 (km s^{-1})	γ (km s^{-1})	rms$_{1,2}$ (km s^{-1})	$M_{1,2}\sin^3 i$ ($\mathcal{M}_\odot$)
49442	Ab1,Ab2	164.55	60023.87	0.317	273.3	24.36	24.91	...	0.37	0.87
		±0.07	±0.65	±0.007	±1.5	±0.27	±0.29	...	0.16	0.85
49442	Aa,Ab	12306	59624.4	0.285	335.5	8.09	4.76	−12.34	0.65	0.92
		±1337	±183	±0.052	±7.2	±0.40	±0.34	±0.28	...	1.56
55691	Aa,Ab	873.14	60792.60	0.8802	355.83	13.16	...	3.77	0.024	0.74:
		±0.54	±0.05	±0.0003	±0.12	±0.04	...	±0.08	...	0.36
61465	Ba,Bb	86.814	60049.67	0.233	130.6	27.62	35.02	−13.59	0.058	1.13
		±0.014	±0.16	±0.002	±0.7	±0.04	±0.06	±0.02	0.093	0.90
78662	Ca,Cb	0.82346	60556.5799	0	0	106.98	124.70	−9.99	0.85	0.57
		±0.00001	±0.0014	fixed	fixed	±1.16	±2.09	±0.72	11.33	0.50
GKM0	Aa1,Aa2	120.74	60637.02	0.381	225.0	21.98	23.71	14.69	0.054	0.83
		±0.18	±0.15	±0.002	±0.6	±0.09	±0.09	±0.03	0.075	0.77
GKM1	Aa1,Aa2	36.589	57373.93	0.40	79.35	13.94	...	28.92	0.11	0.71:
		fixed	fixed 6	fixed	fixed	±0.96	...	±0.55	...	>0.21
GKM2	Aa1,Aa2	11.5155	60779.338	0.030	91.6	31.51	...	96.31	0.16	0.50:
		±0.0002	±0.432	±0.003	±13.6	±0.26	...	±0.08	...	>0.28
GKM4	Aa1,Aa2	305.895	60761.48	0.235	76.2	1.69	...	41.57	0.01	1.0:
		fixed	±9.43	±0.036	±11.7	±0.06	...	±0.05	...	>0.05
GKM5	Aa1,Aa2	28.5546	57400.8229	0.498	208.56	10.49	...	8.96	0.37	0.71:
		fixed	fixed	fixed	fixed	fixed	...	±0.05	...	>0.11
GKM6	Aa1,Aa2	52.0385	60126.228	0.125	57.73	17.57	...	−23.04	0.09	0.98:
		fixed	±0.026	fixed	fixed	±0.06	...	±0.04	...	>0.37

companions with common proper motion (CPM). However, the RV variability could be caused by the resolved source structure, leading to spurious spectroscopic orbits (B. Holl et al. 2023). A few ground-based RV measurements can resolve this issue, and seven such candidates are tested here. The spectral types of these stars range from G to M, and they are called GKM for brevity.

The data and methods, similar to those in the previous papers of this series, are recalled briefly in Section 2. The four solar-type hierarchies are discussed individually in Section 3, and Section 4 reports the test of Gaia orbits in seven potential quadruples. A short discussion in Section 5 closes the paper.

2. DATA AND METHODS

Observations, data reduction, and orbit calculation were described in previous papers of this series (e.g. A. Tokovinin 2022). To avoid repetition, only a brief outline is given here. The CHIRON fiber-fed optical spectrometer (A. Tokovinin et al. 2013; L. A. Paredes et al. 2021) on the 1.5 m telescope at Cerro Tololo was used. This facility is operated by the SMARTS consortium,[2] and the observations are conducted in queue mode. Reduced spectra with a resolution of 80,000 or 28,000 (depending on the target brightness) are cross-correlated with a binary mask based on the solar spectrum. The resulting cross-correlation function (CCF) contains one or more dips encoding the RV, the line width, and the relative flux of each component. Examples of the CCFs are provided in the next Section.

The orbital elements and their errors are determined by the least-squares fits with weights inversely proportional to the adopted RV errors. The IDL code `orbit`[3] was used (A. Tokovinin 2016). When feasible, the inner and outer orbits were fitted jointly with the help of `orbit3` (A. Tokovinin & D. W. Latham 2017).[4] Table 1 lists the spectroscopic elements. Its first two columns identify the system and the component's pair. Then follow the orbital elements in standard notation (period P, epoch of periastron T, eccentricity e, longitude of periastron ω_A of the primary component, RV amplitudes K_1 and K_2, and the systemic velocity γ). The formal errors of the elements determined by the least-squares fit are listed in the following line. The last two columns give the weighted rms residuals to the orbit and the projected masses $M\sin^3 i$ for the primary and secondary components of double-lined binaries (SB2) or the estimated mass of the primary star with colons and the minimum

[2] http://www.astro.gsu.edu/~thenry/SMARTS/

[3] Codebase: http://www.ctio.noirlab.edu/~atokovin/orbit/ and https://doi.org/10.5281/zenodo.61119

[4] Codebase: http://dx.doi.org/10.5281/zenodo.321854

Table 2. Visual Orbits

HIP	System	P (yr)	T (yr)	e	a (arcsec)	Ω_A (deg)	ω_A (deg)	i (deg)
49442	Aa,Ab	33.7	2022.12	0.285	0.208	5.2	335.5	80.3
		±3.7	±0.50	±0.052	±0.010	±0.5	±7.2	±0.6
55691	Aa,Ab	2.3905	2025.3185	0.8802	0.1591	77.4	355.8	56.4
		±0.0015	±0.0001	±0.0003	±0.0003	±0.1	±0.1	±0.6
55691	A,B	414.8	1918.36	0.672	5.819	76.6	16.3	49.8
		±7.8	±0.29	±0.006	±0.041	±0.6	±1.0	±0.6

secondary mass for single-lined orbits (SB1). Complementary data on the visual orbital elements are provided in Table 2, where some spectroscopic elements are duplicated, expressing periods and periastron epochs in Julian years. The position angle of the ascending node Ω_A and the longitude of periastron ω_A refer to the primary component.

The individual RVs and their residuals to the orbits are listed in Table 3, published in full electronically. The RV errors are assigned based on the residuals, and poor data have inflated errors to reduce their weight in the orbit fit. The errors depend on the CCF width and contrast, signal to noise ratio in the spectrum, and blending with other components. For stars without orbits and for components with constant RV, no residuals are given.

3. SOLAR-TYPE STARS

The four solar-type hierarchical systems studied here are presented in Table 4. The data are collected from Simbad and GDR3 (Gaia Collaboration et al. 2021a), the RVs are determined in this work. The first column gives the Washington Double Star (WDS, B. D. Mason et al. 2001) code based on the J2000 coordinates. The HIP and HD identifiers, spectral types, photometric and astrometric data refer either to the individual stars or to the unresolved subsystems. Parallaxes potentially biased by subsystems are marked by colons or relaced by dynamical parallaxes computed from the orbits; asterisks indicate proper motions (PMs) from T. D. Brandt (2021).

In the RV plots in this Section, green squares denote the primary component, blue triangles denote the secondary component, while the full and dashed lines plot the orbit. Typical error bars are smaller than the symbols. Masses of stars are estimated from absolute magnitudes using standard main-sequence relations from M. J. Pecaut & E. E. Mamajek (2013). Orbital periods of wide pairs are evaluated statistically from their projected separations (see A. Tokovinin 2018). Semimajor axes of spectroscopic subsystems are computed using the third Kepler's law.

3.1. *HIP 49442 (Quadruple)*

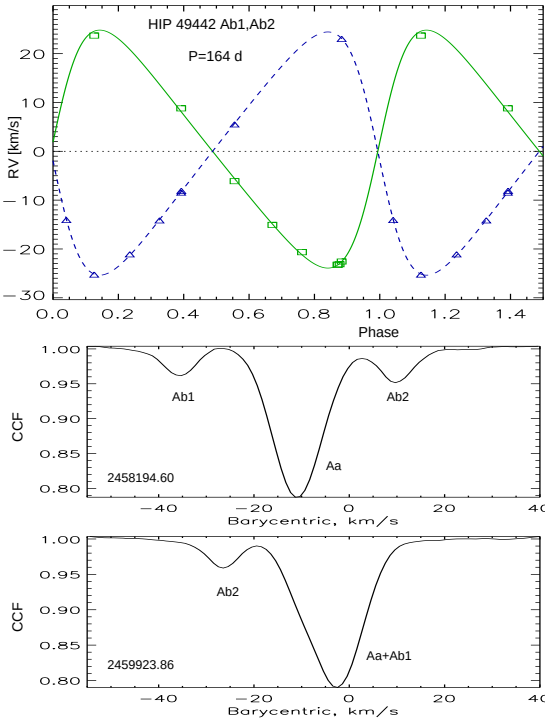

Figure 1. Spectroscopic orbit of HIP 49442 Ab1,Ab2 (top, motion in the orbit of Aa,Ab is subtracted) and two representative CCFs of star A recorded in 2018 and 2022.

This nearby (72 pc) star was resolved by J. Herschel in 1837 into a 3″ visual binary (HJ 4310) with $\Delta V = 0.70$ mag. The estimated period of A,B is about 3 kyr, and in two centuries the separation has increased to 4.″35. The astrometric acceleration of the brighter component A has been detected by Hipparcos and confirmed by Gaia (RUWE of 9.2 and 0.9 for A and B, respectively); T. D. Brandt (2021) determined a large PM anomaly of $(2.7, 25.2)$ mas yr^{-1}. The speckle-interferometric survey of nearby stars with accelerations resolved in 2014 star

Table 3. Radial Velocities and Residuals (fragment)

HIP	System	Date	RV	σ	(O−C)	Comp.
GKM		(JD -2,400,000)	(km s^{-1})			
49442	Ab1,Ab2	58194.6041	−35.743	0.350	0.021	a
49442	Ab1,Ab2	58194.6041	9.858	0.350	−0.057	b
49442	Aa,Ab	58194.6041	−10.837	0.400	0.078	c
49442	Ab1,Ab2	59923.8602	−9.487	0.350	0.680	a
49442	Ab1,Ab2	59923.8602	−26.735	0.350	−0.162	b
49442	Aa,Ab	59923.8602	−3.289	1.000	−1.049	c

(This table is available in its entirety in machine-readable form).

Table 4. Basic Parameters of Observed Multiple Systems

WDS	Comp.	HIP	HD	Spectral	V	$V-K_s$	μ^*_α	μ_δ	RV	ϖ^a
(J2000)				Type	(mag)	(mag)	(mas yr^{-1})		(km s^{-1})	(mas)
10056−8405	A	49442	88948	F8V	7.00	1.69	−107*	0*	−12.3	13.49: DR3
	B	...	...	...	8.38	2.05	−110	−3	−13.8	13.91 DR3
11247−6139	A	55691	99279	K5V	7.54	2.99	−499*	77*	3.8	86.2 dyn
	B	...	...	...	8.60	3.44	−557	89	5.5	85.61 DR3
12357−1201	A	61466	109556	G0	7.88	1.08	−147	18	−11.8	11.72 DR3
	B	61465	...	...	8.27	1.25	−145*	20*	−13.6	11.49: DR3
16035−5747	AB	78662	143474	A7IV	4.63	0.53	−120	−78	−14.0	24.67 dyn
	C	...	...	...	8.02	2.00	−117	−85	−10.0	24.31 DR3

Proper motions and parallaxes are from Gaia DR3 (Gaia Collaboration et al. 2021a). Colons mark parallaxes biased by subsystems, asterisks mark PMs from T. D. Brandt (2021).

Table 5. Positional Measurements and Residuals

HIP	System	t	θ	ρ	σ	O−C$_\theta$	O−C$_\rho$
		(yr)	(°)	(″)	(″)	(°)	(″)
49442	Aa,Ab	2025.2064	191.3	0.1403	0.0020	-0.4	0.0002
49442	Aa,Ab	2025.2064	191.6	0.1400	0.0020	-0.1	-0.0001
55691	Aa,Ab	2024.1541	255.1	0.2987	0.0010	-0.2	0.0001
55691	Aa,Ab	2025.0892	272.9	0.1340	0.0010	-0.0	-0.0017
55691	Aa,Ab	2025.1898	287.8	0.0778	0.0090	6.4	-0.0077
55691	Aa,Ab	2025.2064	282.8	0.0756	0.0050	-1.2	-0.0001

(This table is available in its entirety in machine-readable form)

A as a 0.″18 pair TOK 396 Aa,Ab (A. Tokovinin et al. 2015). The magnitude difference between Aa and Ab is 1.33 and 1.38 mag in bands I and y, respectively. The pair has closed down below the resolution limit after 2018 and opened up again in 2020, after passing through a conjunction. A preliminary 35-yr visual orbit of Aa,Ab computed by the author in 2022 is updated here using both position measurements and RVs.

The RV of this object was found to be variable by B. Nordström et al. (2004), without discrimination between visual components. The spectrum of star A taken in 2018 with CHIRON revealed triple lines, indicating that star Ab is a close pair Ab1,Ab2 (Figure 1). Thus, this system is a quadruple of 3+1 hierarchy. The object was neglected in the following years, and its observations with CHIRON resumed in 2022. In the meantime, the

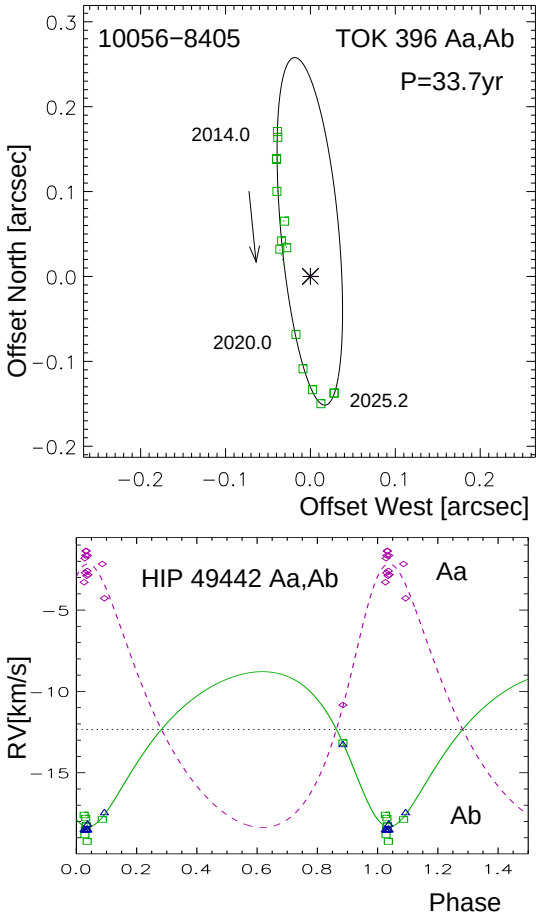

Figure 2. Orbit of HIP 49442 Aa,Ab: speckle measurements (top) and RVs (bottom). In the RV plot, the green line corresponds to the center of mass of Ab, the RVs of Ab1 and Ab2 are plotted by the squares and triengles with the inner orbit subtracted. The dashed magenta curve and diamonds depict the RVs of Aa.

RV of Aa has increased from −10.8 to −2 km s^{-1} owing to its motion in the intermediate orbit. Its dip now overlaps with the weaker dips of Ab1 or Ab2, and for this reason most spectra look double-lined. The RV of star B, measured three times, appears to be constant at −13.8 km s^{-1}. The 4.″35 separation between A and B requires accurate guiding to prevent mixing of their light in the fiber.

Determination of the orbit of Ab1,Ab2 is complicated because both dips are equal. We do not know which of the two weak dips is blended with Aa and which is separated. Regular monitoring helped to associate the dips with correct components and to determine an orbit with a period of 164 days was derived (Figure 1).

The final iteration on the orbits of Aa,Ab and Ab1,Ab2 was made by a joint fit using `orbit3`. The orbit of Aa,Ab is illustrated in Figure 2, and its visual elements are given in Table 2. The position measurements are made by speckle interferometry at the 4.1 m Southern Astrophysical Research (SOAR) telescope. The data before 2024 are published in (A. Tokovinin et al. 2024) and previous papers of this series. More recent measurements are listed in Table 5 (its electronic version contains all SOAR measurements). The partial speckle and RV coverage leaves considerable uncertainty in the period and other elements. The mass sum of 2.7 $M_\odot$ derived from the Aa,Ab orbit and the unbiased GDR3 parallax of star B, 13.91 mas, agrees with the spectroscopic masses of 1.0 and 1.68 $M_\odot$ for Aa and Ab, respectively.

The V magnitudes of Aa, Ab1, and Ab2 are 7.95, 10.08, and 10.08 mag, respectively, based on the speckle photometry and assuming that Ab1 and Ab2 are equal. The spectroscopic masses $M\sin^3 i$ of Ab1 and Ab2 (Table 1) match the masses estimated from the absolute magnitudes. This implies that the orbit of Ab1,Ab2 has a large inclination and suggests its possible alignment with the orbit of Aa,Ab. However, the estimated mass of Aa, 1.26 $M_\odot$, which agrees with its spectral type F8V, is larger than 1 $M_\odot$ derived from the combined orbit of Aa,Ab. Further observations will eventually yield more accurate measurement of all masses.

The angular semimajor axis of Ab1,Ab2 is 9.8 mas, so, despite the large inclination, the innermost pair can be marginally resolved by speckle interferometry at 8 m telescopes. Such a resolution would determine the mutual inclination between Aa,Ab and Ab1,Ab2. Owing to the near-equality of Ab1 and Ab2, the wobble in the outer orbit is too small to be detectable. The residuals of the speckle measures of Aa,Ab to the orbit are about 1 mas. The relatively large residuals in the RVs of Aa are caused by frequent blending of its CCF dip with the dips of Ab1 or Ab2.

The lithium 6707Å line is clearly detectable in the spectra of Aa and B, indicating that this system is juvenile. The dips of Aa and B are slightly widened by rotation ($V\sin i$ or 6.8 and 4.0 km s^{-1}, respectively), while the lines of Ab1 and Ab2 do not exhibit any measurable rotational broadening.

3.2. *HIP 55691 (Triple)*

This triple system is a close neighbour located at 11.7 pc. The main star A is known as HIP 55691 or GJ 428. The visual companion B has been noted by J. Hershel in 1834 at 4″. Its motion, monitored for almost two centuries, constrains the outer orbit quite well. The pair A,B passed through the periastron in 1918 and slowly opens up, now being separated by 7.″6.

A strong suspiction that star A contains a subsystem was raised by the acceleration, namely the PM anomaly

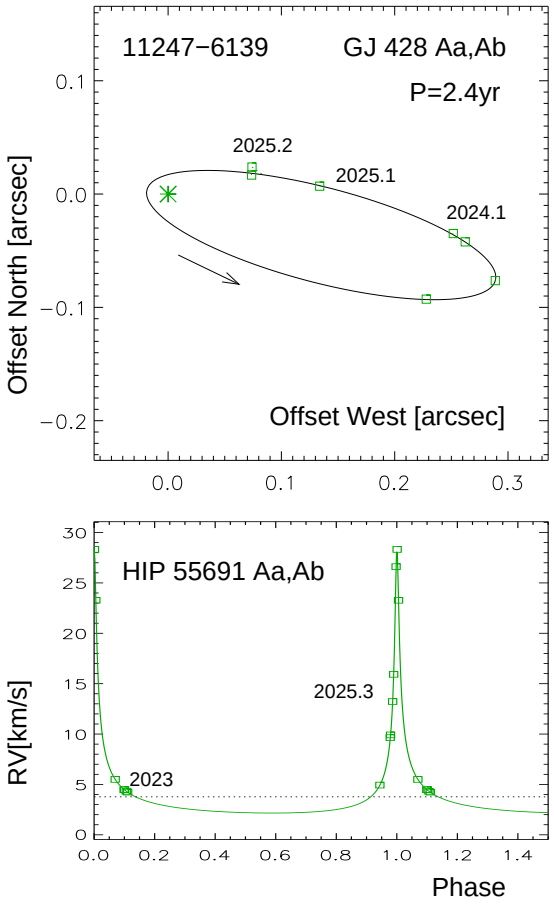

Figure 3. Visual orbit (top) and the RV curve (bottom) of HIP 55691 Aa,Ab.

detected via comparison between Gaia DR2 and Hipparcos by T. D. Brandt (2018) and P. Kervella et al. (2019). The lack of 5-parameter astrometry in GDR3 indicates that the star was probably resolved. Its first observation at SOAR in 2021 revealed a faint ($\Delta I_{\rm Aa,Ab}$ = 3.0 mag) companion Ab at 0.″25 separation (A. Tokovinin et al. 2022). Subsequent monitoring was inconclusive until 2025, when the pair became closer and started to move faster. The speckle data suggested an eccentric orbit with a period of 2.4 yr. Such an orbit would produce a substantial RV variation at periastron, predicted for 2025 April. Spectroscopy with CHIRON in 2025 confirmed this prediction and enabled calculation of the combined spectro-interferometric orbit illustrated in Figure 3. The eccentricity of $e_{\rm Aa,Ab} = 0.8802 \pm 0.0003$ is high, albeit not extreme. Five CHIRON spectra of this star taken in 2023 by T. Johns in a survey of nearby K dwarfs were also used (the RVs were measured by cross-correlation).

The mass of Aa deduced from its absolute magnitude, 0.74 $M_\odot$, is normal for a K5V dwarf. The RV amplitude and the inclination correspond to the mass of Ab of 0.36 $M_\odot$, or a mass sum of 1.10 $M_\odot$; the mass sum computed from the orbit and the parallax is 1.12 $M_\odot$. The amplitude of the photocenter wobble should be about 43 mas; its ratio to the semimajor axis is the wobble factor $f^* = q/(1+q) - r/(1+r) = 0.27$, where $q_{\rm Aa,Ab} = 0.49$ is the mass ratio and $r_{\rm Aa,Ab} = 0.06$ is the flux ratio corresponding to a magnitude difference of 3 mag. No astrometric or spectroscopic orbits are provided in the GDR3, possibly because of insufficient sampling near the periastron. However, the wobble caused by the inner subsystem seriously biases the astrometry of star A in both Hipparcos and Gaia missions. The best (but not perfect) estimate of the PM of A, $(-499.40, 77.46)$ mas yr^{-1}, is obtained by T. D. Brandt (2018) from the Hipparcos and GDR2 positions.

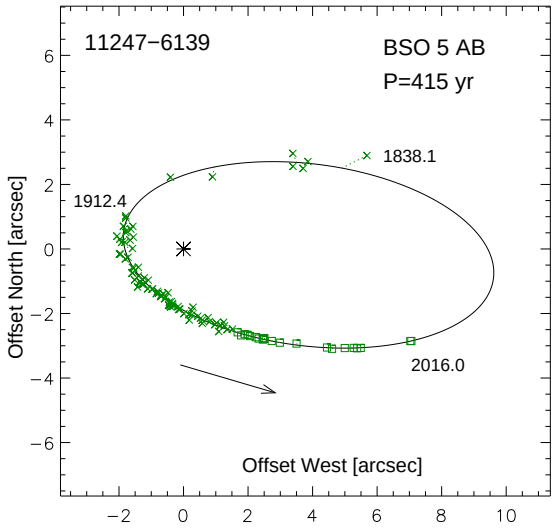

Figure 4. Visual orbit of HIP 55691 A,B (WDS 12247−6139). Crosses mark micrometer measurements, and squares stand for more accurate photographic measurements and space astrometry.

The orbit of the outer pair A,B has been computed and updated several times in the past. I refined its elements (see Table 2) by assigning appropriate errors (hence weights) of 0.″2 to the micrometer measurements, 0.″05 to the photographic measurements after 1950 (the micrometer data after 1950, as well as obvious outliers, are ignored), 10 mas to the Hipparcos position, and 2 mas to the relative position in GDR3. This relatively well-constrained orbit plotted in Figure 4 is similar to the orbit computed by I. S. Izmailov (2019). The weighted rms residuals are 10 mas. Using the accurate GDR3 parallax of star B, 85.61±0.021 mas, the orbit leads to the mass sum of 1.83 $M_\odot$, close to our estimate of 1.74 = 1.10 + 0.64 $M_\odot$. The motion of B relative to A in 2015.5 was $(-54.53 + 12.47)$ mas yr^{-1} according

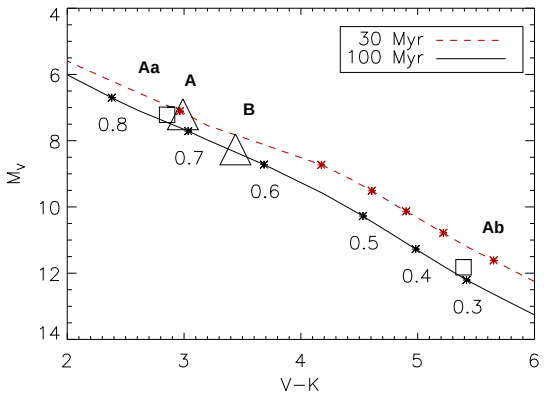

Figure 5. Color-magnitude diagram of HIP 55691. The PARSEC isochrones for 100 and 30 Myr are plotted, with asterisks marking masses from 0.3 to 0.8 $M_\odot$. The positions of stars A and B are marked by large triangles, while smaller squares indicate tentative locations of Aa and Ab.

to this orbit. The difference between PMs of B and A, $(-57.4, +11.1)$ mas yr^{-1}, is in reasonable agreement. Based on the estimated masses of A and B, the center of mass of the system has a PM of $(-522, +81)$ mas yr^{-1}.

The systemic RV of A, 3.77±0.07 km s^{-1}, differs from the three RVs of B measured with CHIRON (mean 5.50±0.02 km s^{-1}) owing to motion in the outer orbit. Fixing the RV amplitude $K_A = 1.72$ km s^{-1} to its estimated value, I obtain $K_B = 3.45$ km s^{-1} and the systemic velocity of 4.32 km s^{-1}. The ascending nodes of both orbits are known without ambiguity, and their mutual inclination is $6\overset{\circ}{.}5 \pm 0\overset{\circ}{.}8$. Similar orientation of inner and outer orbits is notable by comparing Figures 3 and 4. The lines of apsides of both orbits also point in the same direction. Star B has good astrometry in GDR3 (a RUWE of 1.1) and a constant RV, so it does not host inner subsystems, as far as we can tell.

After computing the inner and outer orbits separately, I fitted them jointly using `orbit3`, and the elements given here correspond to this final iteration. The tiny wobble in the motion of A,B does not look convincing on the orbit plot, but the fitted coeficient $f^* = 0.19 \pm 0.03$ is formally significant and comparable to its estimate.

This star has been detected in X-rays and, accordingly, was suspected to be young by C. A. O. Torres et al. (2006). However, the Li 6707Å line is not seen in the CHIRON spectra of Aa and B, and the width of the CCF dips corresponds to a moderate projected rotation $V \sin i$ of 4.3 and 5.6 km s^{-1} for A and B, respectively. The spatial velocity $(U, V, W) = (-24.8, -15.2, -5.3)$ km s^{-1} computed using the estimated motion of the center of mass of AB suggests potential membership in the IC 2391 (Argus) association with an age of ∼50 Myr (T. Nakajima & J.-I. Morino 2012). In Figure 5 the stars are placed on the color-magnitude diagram and compared to two PARSEC isochrones for solar metallicity (A. Bressan et al. 2012). The magnitudes of Aa and Ab are assigned tentatively by assuming masses of 0.74 and 0.36 $M_\odot$, computing the magnitude differences in the V and K bands from the 100 Myr isochrone, and splitting the total flux accordingly. As $\Delta V_{\rm Aa,Ab} = 4.7$ mag is large, the absolute magnitudes M_V of Aa and A=Aa+Ab are almost identical, but Aa is slightly bluer than A. The 100 Myr isochrone predicts a magnitude difference of 3.3 mag in I, close to the measured value (3.0 mag). On the other hand, the masses and the 30 Myr isochrone correspond to a smaller magnitude difference of $\Delta I_{\rm Aa,Ab} = 2.1$ mag, contradicting the observations. Interestingly, the mass of Ab measured from the inner orbit and the magnitude difference, taken together, help us constrain the age of this triple system: about 100 Myr or slightly less. A more refined analysis can be made in the future when relative photometry of Aa,Ab in various bands becomes available.

3.3. *HIP 61466+61465 (Quadruple)*

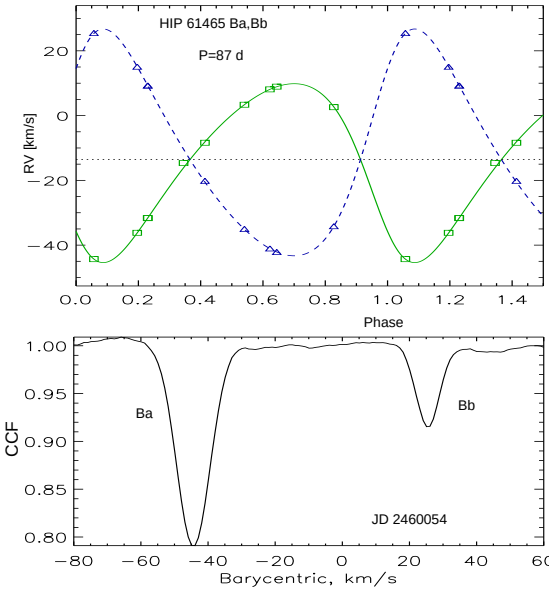

Figure 6. Spectroscopic orbit of HIP 61465 Ba,Bb (top) and the CCF recorded on JD 2,460,054 (bottom).

This hierarchical system located at 85 pc is composed of bright stars A (HIP 41466) and B (HIP 41465) at $27\overset{''}{.}5$ separation. The wide pair STF 1659 has moved very little since its first measurement by W. Struwe in 1828. The WDS lists fainter components C to F, but all these stars are optical, as evidenced by their unstable relative positions, mismatching PMs, and parallaxes.

T. D. Brandt (2021) detected a statistically significant PM anomaly (i.e. a long-term acceleration) of 2 mas yr^{-1} in both stars, suggesting existence of inner subsystems. However, it is known that Hipparcos astrometry of visual binaries with separations on the order of 20″ often has large errors owing to its measurement procedure, so the veracity of the anomaly derived from the Hipparcos positions remains questionable; GDR3 has a RUWE of 1.0 and 3.1 for A and B, respectively.

S. Desidera et al. (2006) measured the RVs of stars A and B on JD 2 447 720.3 at −14.77 and +4.78 km s^{-1}, respectively, and suggested that both can be variable; they have not noticed double lines in the spectrum of B. The RVs of A measured with CHIRON in 2018 and 2023 are −11.83 and −10.77 km s^{-1}. The slow positive RV trend of star A is caused by a subsystem with a long but still unknown period. This pair, presumably responsible for the acceleration, could possibly be resolved by speckle interferometry or adaptive optics.

Double lines in the CHIRON spectrum of star B were noted in 2018. However, the orbit has not been pursued at the time. Additional spectra taken in 2023 confirm the double-lined nature and establish the orbit of Ba,Bb with $P = 86.8$ days (Figure 6). The photocenter motion is a likely cause of the astrometric noise in GDR3.

Comparison between the masses of Ba and Bb estimated from their absolute magnitudes (1.20 and 0.91 $M_\odot$) and the spectroscopic masses $M \sin^3 i$ of 1.16 and 0.97 $M_\odot$ indicates that the orbit of Ba,Bb has a large inclination. The Li line was noted in the spectrum of the brighter component Ba, but it is absent in the spectrum of A.

3.4. *HIP 78662 (Quadruple)*

This is a bright quadruple system. The main star, ι Nor (HR 5961), has a visual companion C at 11″, first noted by John Hershel in 1835 (HJ 4825). Although star C is relatively bright ($V = 8.02$ mag), it has not deserved individual identifies except 2MASS, apparently being lost in the glare of its brighter sister. The latter has been resolved in 1897 as a 0.″8 pair SEE 258, and its visual orbit with $P = 26.84$ yr is very well known. The dynamical parallax of 24.68 mas derived from this orbit and the estimated masses matches well the GDR3 parallax of C, 24.31 mas. As AB is a binary, Gaia did not determine its astrometric parameters, while the Hipparcos parallax of 25.4 mas is less accurate.

Star C was observed with CHIRON in 2018. The spectrum revealed very broad and low-contrast double lines. Considering the likely short period, the low expected accuracy of the RVs, and other targets of higher priority, further study was postponed till 2023. New spectra confirmed the double-lined nature of this star and its rapidly variable RVs. Three representative CCFs in the lower panels of Figure 7 illustrate the dips of unequal amplitudes that swap within a few days. When the dips partially overlap, the CCFs are broad and of irregular shape, so attempts to fit overlapping dips failed, except

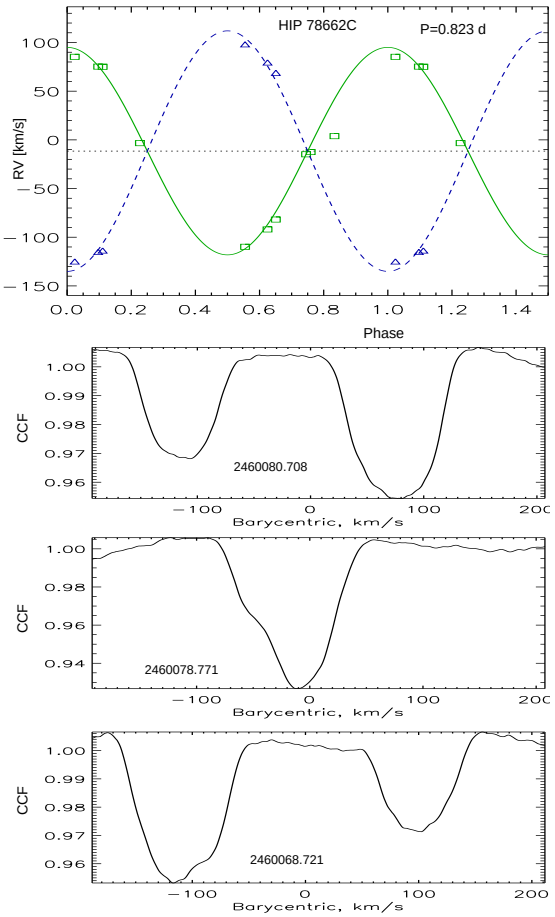

Figure 7. Spectroscopic orbit of HIP 78662 Ca,Cb (top) and three representative CCFs (bottom).

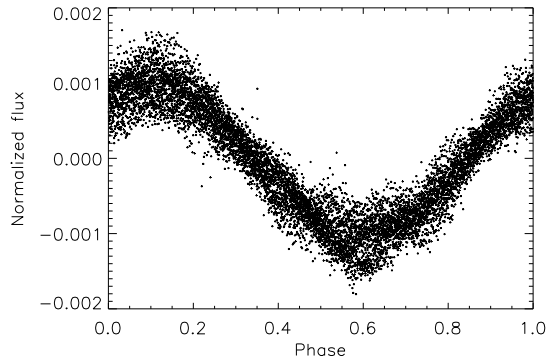

Figure 8. Light curve of HIP 78662C from the TESS Sector 39 folded with a period of 0.81947 days and an arbitrary initial phase.

when the overlap is nearly perfect and the single dip is not too wide, as shown. The orbital period of 0.82 days was confirmed by taking two spectra within a couple of hours on a single night.

A short orbital period suggests possibility of eclipses. The light curves (LCs) of HIP 78662C (TIC 426452677) were retrieved from the TESS (G. R. Ricker et al. 2014) archive for sectors 1 (2018) and 39 (2021), both with a 2 min. cadence. Both data sets show a low-amplitude modulation with dominant periods of 0.41 and 0.82 days in sectors 1 and 39, respectively. The latter has a larger amplitude, and the LC is shown in Figure 8. The LCs refer to the combined light of three stars where the flux is dominated by the brighter components A and B. Although early-type (A7IV) stars A and B might have rapid rotation, they are unlikely to have spots. The light modulation is therefore attributable to the chromospherically active stars Ca and Cb, tidally synchronized with the orbit. The modulation periods are very close to the orbital period and its second harmonic. The irregular shape of the CCF dips is likely caused by the starspots.

The TESS LC clearly shows the lack of eclipses. The same conclusion emerges from the amplitudes of the RV variation that correspond to the projected masses $M \sin^3 i$ of 0.37 and 0.33 $M_\odot$. Comparison with masses estimated from M_V, around 0.9 $M_\odot$, leads to the inclination of 45°. Summarizing, this system is a 2+2 quadruple with very unequal inner periods of 26.8 yr and 0.82 d. If the twin pair Ca,Cb merges, the mass of the resulting blue straggler, 1.75 $M_\odot$, will be similar to the masses of stars A and B, 1.75 and 1.54 $M_\odot$ respectively.

4. TESTING HIERARCHIES WITHIN 100 PC

A large speckle survey of candidate hierarchical systems within 100 pc derived from the Gaia GCNS (Gaia Collaboration et al. 2021b) enabled confirmation of a few hundred triples where the wide outer pair consists of two Gaia sources, and the inner pair, resolved by speckle interferometry, is revealed by the Gaia multiplicity indicators (A. Tokovinin 2023a). In several cases, the NSS (Gaia Collaboration et al. 2023) contains orbits of resolved inner pairs. Twenty such systems are listed in Table 3 of A. Tokovinin (2023a).

Some of the NSS binaries coincide with the close speckle pairs because the orbital periods inferred from the separation, P^*, match the NSS periods. These cases are confirmed by subsequent speckle monitoring, allowing calculation of several visual (resolved) orbits (A. Tokovinin et al. 2024). However, in the remaining cases the NSS periods $P_{\rm NSS}$ are much shorter than P^*. If the NSS orbits are verified, these would be quadruple systems of 3+1 hierarchy (a close NSS pair, an intermediate speckle pair, and the outer companion resolved by Gaia).

However, the NSS spectroscopic orbits of close pairs require confirmation. Gaia measured the RVs by a slitless spectrometer with a spectral resolution of 11,500. The RV depends on the source position along the scan determined by the astrometric solution; an offset of 1″ corresponds to an RV offset of 146 km s^{-1}. Presence of a close companion can bias the RVs in several ways, leading to false spectroscopic orbits, as described in section 3.3 of B. Holl et al. (2023). A companion separated by ρ from 0.″1 to 0.″9 can be resolved in scans along the binary direction, and in such case the Gaia astrometry refers to the main star (which also dominates in the spectrum). However, in other scans that are nearly perpendicular to the binary, the components are blended in the common Gaia window, and the astrometry refers to the photocenter. Mixture of resolved and unresolved scans degrades the quality of Gaia astrometry, causing an increased RUWE. The RVs are also biased. If the flux ratio in the Gaia radial velocity spectrometer band (at 870 nm) is r, the shift between the primary star position and the photocenter is $\rho r/(1+r)$, and the corresponding RV bias can reach a few km s^{-1}. An example of spurious NSS SB1 orbit with an amplitude of ∼9 km s^{-1} for a 0.″3 binary is given in Figure 14 of B. Holl et al. (2023). For unresolved point-like sources such as astrometric binaries, the photocenter motion (not accounted for in the Gaia spectroscsopic orbits) also produces RV errors and biases the elements, albeit not dramatically.

The Gaia scan direction changes with a period of ∼63 days. Spurious signals caused by the source structure might appear periodic, with a range of possible periods; the 31.5 day spurious period is one of the strongest (B. Holl et al. 2023). Speckle companions (except the closest) move little during the 3 yr time span of GDR3, so the companion-induced RV errors should be related mostly to the scan direction.

If some NSS orbits of stars with speckle companions are spurious, they are not 3+1 quadruples, just triples. To test the orbits, RVs of seven candidate stars were monitored with CHIRON. These stars are given here short names from GKM0 to GKM5. The last object, HIP 58691 (HD 104532), is relatively bright (V = 9.26 mag); it is denoted here as GKM6. The WDS-like codes and other data of these stars are reported in Table 6. It contains the Gaia NSS solution type, its period $P_{\rm NSS}$, and the RV semiamplitude $K_{\rm NSS}$. The following columns give the separation ρ, the magnitude difference ΔI, and the estimated periods P^* of the speckle companions. The separations and magnitude differ-

Table 6. Stars with NSS Orbits and Speckle Companions

GKM	WDS	DR3	Sol.	$P_{\rm NSS}$ (d)	$K_{\rm NSS}$ (km s^{-1})	ρ ($''$)	ΔI (mag)	P^* (yr)	Comment
0	04097−5256	4780342550850239872	AORB	121.9	...	0.176	3.4	38	SB2
1	07543+0232	3088161818892312704	SB1	36.6	15.2	0.364	2.3	155	Confirmed
2	09336−2752	5633969259436187648	SB2	37.2	37.6	0.139	2.9	13	$P = 11.5$d
3	15397−4956	5985420622174761600	SB1	44.8	10.0	0.046	0.8	5	RV const.
4	20147−7252	6373829259376877440	SB1	305.9	2.2	0.253	3.5	75	Confirmed
5	21460−5233	6462355265559115392	SB1	28.6	10.5	0.088	2.5	16	Confirmed
6	12022−4844	6130627011126533760	SB1	52.0	16.7	0.095	3.1	13	Confirmed

ences correspond to potential spurious RV amplitudes 146 $\rho r/(1+r)$ of 1–2 km s^{-1}, except GKM0 where it reaches 5.7 km s^{-1}. The visual magnitudes of the first six stars range from 9.4 to 12.6, and they were observed in the fiber mode with a spectral resolution of 28,000, while HIP 58691 (GKM6) was observed in the slicer mode with a resolution of 80,000.

The original intent was to measure only a few RVs of each star for a quick verification of the GDR3 orbits. Some stars, however, required additional observations. Observations with CHIRON started in 2023. They were stopped for administrative reasons in 2023 September and resumed a year later, in 2024 August. The pause has seriously impacted this program, precluding optimum time coverage. Figure 9 gives the RV curves deduced from the CHIRON spectra. Individual systems are commented below, and their hierarchical structure is illustrated in Figure 10. There are five quadruples of 3+1 architecture, one quintuple, and one triple.

GKM0 (CD−53 862) is revealed as an SB2 with a 120.7 day period (Table 1) which matches the Gaia astrometric orbit with a period of 121.9 days. Gaia did not determine the SB2 orbit possibly because of insufficient spectral resolution. All elements of the spectroscopic orbit are fitted without restrictions. The RV amplitudes and inclination lead to the masses of 0.83 and 0.77 $M_\odot$ (mass ratio $q = 0.93$). The areas of the CCF dips give the flux ratio of $r = 0.68$, so the V magnitudes of spectroscopic components Aa1 and Aa2 are 10.51 and 10.93 mag, respectively, and their absolute magnitudes match the measured masses. The full semimajor axis of this orbit is 6.6 mas, while the axis of the Gaia astrometric orbit is 0.7 mas. Owing to the blending, the astrometric amplitude should be reduced by the factor $f^* = q/(1+q) - r/(1+r) = 0.08$, close to the actual ratio of 0.1. If blending is neglected, the astrometric orbit gives the mass ratio of ∼0.15. The faint ($\Delta I = 3.4$ mag) speckle companion at $0\farcs176$ has an estimated period P^* of 38 yr, and some orbital motion is detected in two years; its mass is comparable to the masses of Aa1 and Aa2. The CPM companion B at $36\farcs6$ has an estimated mass of 0.24 $M_\odot$. This is a genuine 3+1 quadruple.

GKM1 has a variable RV, and the 4 available CHIRON observations match the 36.6 day Gaia SB1 orbit (I fixed its elements and fitted only the RV amplitude and the systemic velocity). The Gaia orbit is plotted by dashed line in Figure 9. With the Aa1 mass of 0.71 $M_\odot$, the minimum mass of the spectroscopic secondary Aa2 is 0.21 $M_\odot$. The speckle companion Ab at $0\farcs36$ and 2.3 mag fainter than Aa ($P^* \sim 154$ yr) is confirmed indirectly by the multi-peak transits of star A in Gaia. Two more Gaia stars B and C, making a $1\farcs3$ pair, are located at $153''$ from A and have common PM and parallax. The estimated masses of B and C, 0.7 and 0.4 $M_\odot$, are comparable to the mass of Aa1. The projected separation between A and BC is 14 kau, and the estimated outer period is ∼1 Myr. Therefore, this a 3+2 quintuple system with a total mass around 2.6 $M_\odot$.

GKM2 (LP 902-100) has an SB2 orbit in the NSS with a period of 37.17 days, amplitudes of 37.55 and 35.66 km s^{-1}, and a systemic velocity of 96.4 km s^{-1}. Only single lines are seen in the CHIRON spectra, however. The RV is definitely variable and corresponds to a quasi-circular orbit with a period of 11.5 days and an amplitude of 31.5 km s^{-1}. Both the amplitude and the systemic velocity are similar to their values in the GDR3 orbit, while the periods differ dramatically. However, the GDR3 period aliased by the 63 day Gaia scanning cycle corresponds to twice the actual period: 1/37.17 + 1/63 = 1/23.4. One might suspect that the Gaia pipeline for spectroscopic orbits measured only single RVs in each scan but, somehow, alternatively assigned them to two spectroscopic components, thus leading to a false orbit with double (and, furthermore, aliased) period and comparable RV amplitudes. The speckle companion has been discovered in 2021.9 at $0\farcs139$ separation ($P^* \sim 13$ yr), and its fast motion is indeed detected by two subsequent observations in 2024 and 2025 (the

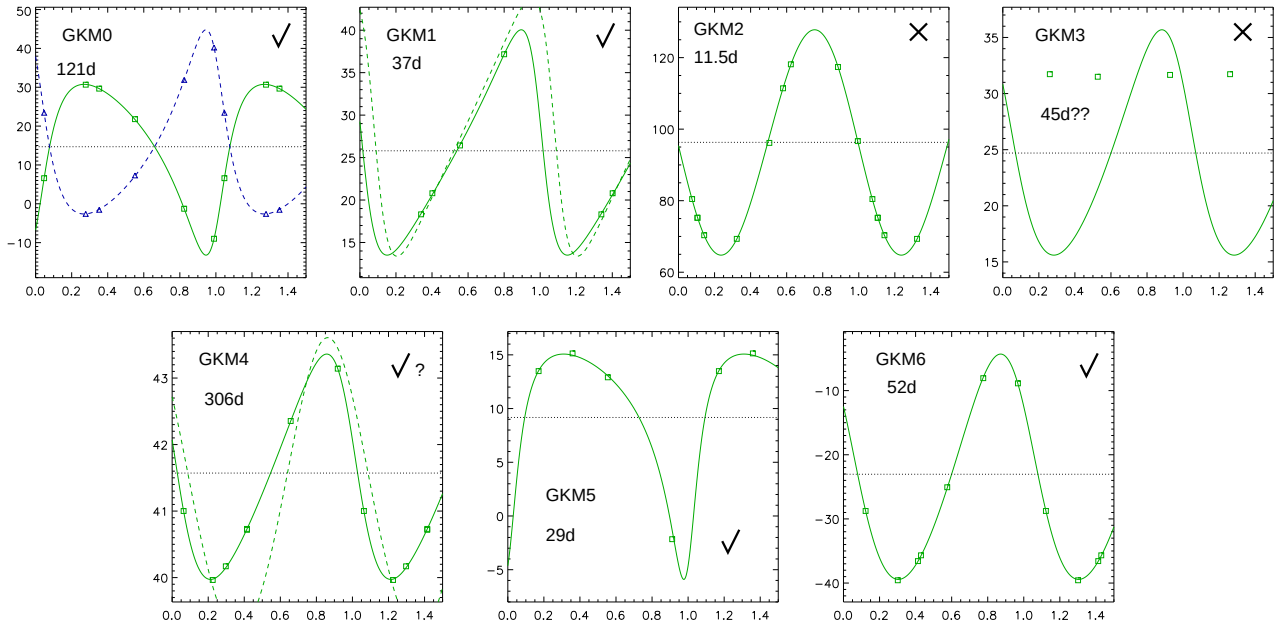

Figure 9. RV curves of seven GKM stars observed with CHIRON (see text). Confirmed Gaia periods are marked by ticks, unconfirmed — by crosses. The RVs of primary and secondary components are plotted by squares and triangles, respectively, the fitted orbits by full lines, and some GDR3 orbits by dashed lines.

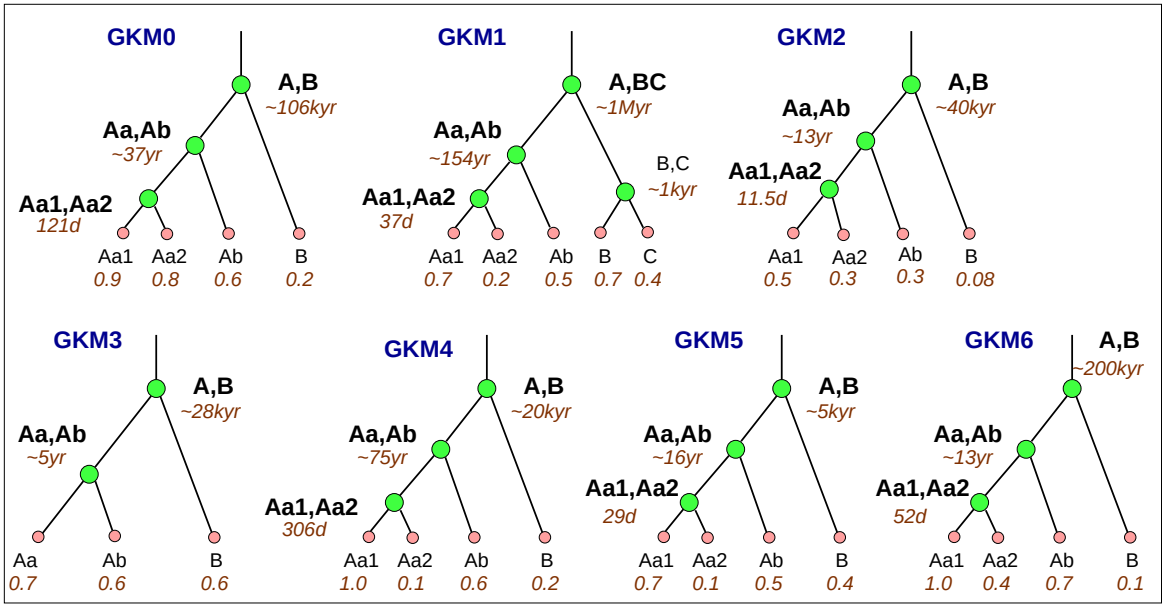

Figure 10. Architecture of seven GKM systems. Green circles show subsystems (their known or estimated periods are given), small pink circles — individual stars; their approximate masses are shown below.

position angle has changed by 77°). The magnitude difference is $\Delta I \approx 2.9$ mag, so the companion cannot explain the double-lined Gaia orbit. The faint CPM star B at 29″ has estimated mass of 0.08 $M_\odot$ and a spectral type M7.5 (DEA 21 pair in the WDS). So, this is a 3+1 quadruple where the Gaia SB2 orbit is spurious.

GKM3 (TYC 8304-794-1) has a constant RV of 31.6 km s^{-1} (3 measurements). The RV amplitude of the Gaia 45 day orbit is 10.0 km s^{-1}, the systemic RV is 24.7 km s^{-1}; this orbit is proven here to be spurious. The speckle companion at 0.″045 ($\Delta I \sim 0.8$ mag) has a period on the order of 5 yr; this pair has closed down in 2022–2023 and was unresolved in 2024.18. If its orbit is eccentric, a large RV variation could possibly be detected by Gaia and interpreted with a wrong period.

Star B is at 15.″6. This system is only a triple with component's masses between 0.6 and 0.7 $M_\odot$.

GKM4 (CD−73 1491, $V = 9.41$ mag) is the brightest target in this group. The 306 day Gaia orbit is confirmed by CHIRON, despite its small amplitude of 2.2 km s^{-1} . The CHIRON orbit fitted to 7 RVs (with the fixed Gaia period) has a larger eccentricity and an amplitude of 1.8 km s^{-1} , with a roughly matching systemic velocity. The Gaia SB1 orbit, plotted by dashed line in Figure 9, is likely biased by the scan-dependent RV errors with an estimated amplitude of 1.4 km s^{-1} caused by the speckle companion; the orbit would be considered spurious if it were not confirmed. The spectroscopic secondary Aa2 has a minimum mass of 0.05 $M_\odot$, in the substellar domain. The speckle companion at 0.″253 with $\Delta I = 3.5$ mag has a period of ∼75 yr (its motion is detected) and the estimated mass of 0.6 $M_\odot$. The CPM companion B at 19.″7 has a mass of 0.16 $M_\odot$. So, the solar-mass star Aa1 has three low-mass companions arranged in a 3+1 hierarchy.

GKM5: The four CHIRON RVs match the 28.55 day Gaia orbit (only the systemic velocity γ was adjusted by 1.65 km s^{-1}). The minimum mass of the spectroscopic secondary Ab is 0.11 $M_\odot$. The speckle companion is at 0.″09 ($P^* \sim 16$ yr, the orbital motion is detected), and the CPM companion B is at 4.″25. This is a 3+1 quadruple composed of K- and M-dwarf stars.

GKM6 (HIP 58691, HD 104532) was observed 7 times, and the RVs match the GDR3 orbit. I fitted the elements T, K_1, and V_0 while fixing the remaining elements to the respective GDR3 values. The rms residuals are 0.09 km s^{-1} .

5. DISCUSSION

The Gaia mission was designed to deal with single stars and binaries. Hierarchical systems are obvious troublemakers for the automated Gaia pipelines that cannot take into account such aspects as spatial and spectral blending between components, the cross-talk between spatial and spectral domains, and multiple periods. The Gaia scanning law limits the range of accessible periods and the phase coverage, especially for very short periods or very eccentric orbits. Although clever ways to circumvent these problems might be invented in the future, the need of complementary data on hierarchical systems to pinpoint their true architecture is obvious.

The four solar-type hierarchies studied here, as well as other targets of this project (A. Tokovinin 2023b), illustrate the complexity and diversity of situations, unlikely to be handled properly by the automatic pipelines. On the other hand, the immense discovery potential of Gaia is evident, especially for stars brighter than $G \sim 13.5$ mag that have the RV data. An RV variability in excess of the orbital motion expected in the astrometric binaries revealed hundreds of new candidate hierarchies whose inner periods remain unknown (D. Bashi & A. Tokovinin 2024). This resembles the pre-Gaia situation when the survey of B. Nordström et al. (2004) discovered new hierarchies, but further dedicated monitoring was needed to establish their architecture.

Among the seven stars with NSS orbits and speckle companions tested here, six are 3+1 (or 3+2) hierarchies, while GKM3 is only a triple. The NSS orbits of GKM2 and GKM3 are not confirmed. The results of this study are incorporated in the multiple star catalog (A. Tokovinin 2018).[5]

ACKNOWLEDGMENTS

I thank the operators of the 1.5 m telescope for executing observations of this program and the SMARTS team for scheduling and pipeline processing. T. Johns has kindly shared the spectra of HIP 55691 taken in 2023 with CHIRON and used here in the orbit fit. Comments by D. Bashi and B. Mason on the draft version of this paper are greatly appreciated.

The research was funded by the NSF's NOIRLab. This work used the SIMBAD service operated by Centre des Données Stellaires (Strasbourg, France), bibliographic references from the Astrophysics Data System maintained by SAO/NASA, and the Washington Double Star Catalog maintained at USNO. This work has made use of data from the European Space Agency (ESA) mission Gaia (https://www.cosmos.esa.int/gaia), processed by the Gaia Data Processing and Analysis Consortium (DPAC, https://www.cosmos.esa.int/web/gaia/dpac/consortium). Funding for the DPAC has been provided by national institutions, in particular the institutions participating in the Gaia Multilateral Agreement. This paper includes data collected with the TESS mission, obtained from the MAST data archive at the Space Telescope Science Institute (STScI). Funding for the TESS mission is provided by the NASA Explorer Program. STScI is operated by the Association of Universities for Research in Astronomy, Inc., under NASA contract NAS 526555.

Facility: CTIO:1.5m, SOAR, Gaia

REFERENCES

Bashi, D., Shahaf, S., Mazeh, T., et al. 2022, MNRAS, 517, 3888, doi: 10.1093/mnras/stac2928

Bashi, D., & Tokovinin, A. 2024, A&A, 692, A247, doi: 10.1051/0004-6361/202452637

Brandt, T. D. 2018, ApJS, 239, 31, doi: 10.3847/1538-4365/aaec06

Brandt, T. D. 2021, ApJS, 254, 42, doi: 10.3847/1538-4365/abf93c

Bressan, A., Marigo, P., Girardi, L., et al. 2012, MNRAS, 427, 127, doi: 10.1111/j.1365-2966.2012.21948.x

Czavalinga, D. R., Mitnyan, T., Rappaport, S. A., et al. 2023, A&A, 670, A75, doi: 10.1051/0004-6361/202245300

Desidera, S., Gratton, R. G., Lucatello, S., Claudi, R. U., & Dall, T. H. 2006, A&A, 454, 553, doi: 10.1051/0004-6361:20064895

Gaia Collaboration, Brown, A. G. A., Vallenari, A., et al. 2016, A&A, 595, A2, doi: 10.1051/0004-6361/201629512

Gaia Collaboration, Brown, A. G. A., Vallenari, A., et al. 2021a, A&A, 649, A1, doi: 10.1051/0004-6361/202039657

Gaia Collaboration, Smart, R. L., Sarro, L. M., et al. 2021b, A&A, 649, A6, doi: 10.1051/0004-6361/202039498

Gaia Collaboration, Arenou, F., Babusiaux, C., et al. 2023, A&A, 674, A34, doi: 10.1051/0004-6361/202243782

Gosset, E., Damerdji, Y., Morel, T., et al. 2025, A&A, 693, A124, doi: 10.1051/0004-6361/202450600

Holl, B., Fabricius, C., Portell, J., et al. 2023, A&A, 674, A25, doi: 10.1051/0004-6361/202245353

Izmailov, I. S. 2019, Astronomy Letters, 45, 30, doi: 10.1134/S106377371901002X

Kervella, P., Arenou, F., Mignard, F., & Thévenin, F. 2019, A&A, 623, A72, doi: 10.1051/0004-6361/201834371

Kirkpatrick, J. D., Marocco, F., Gelino, C. R., et al. 2024, ApJS, 271, 55, doi: 10.3847/1538-4365/ad24e2

Mason, B. D., Wycoff, G. L., Hartkopf, W. I., Douglass, G. G., & Worley, C. E. 2001, AJ, 122, 3466, doi: 10.1086/323920

Nakajima, T., & Morino, J.-I. 2012, AJ, 143, 2, doi: 10.1088/0004-6256/143/1/2

Nordström, B., Mayor, M., Andersen, J., et al. 2004, A&A, 418, 989, doi: 10.1051/0004-6361:20035959

Paredes, L. A., Henry, T. J., Quinn, S. N., et al. 2021, AJ, 162, 176, doi: 10.3847/1538-3881/ac082a

Ricker, G. R., Winn, J. N., Vanderspek, R., et al. 2014, in Society of Photo-Optical Instrumentation Engineers (SPIE) Conference Series, Vol. 9143, Space Telescopes and Instrumentation 2014: Optical, Infrared, and Millimeter Wave, ed. J. Oschmann, Jacobus M., M. Clampin, G. G. Fazio, & H. A. MacEwen, 914320, doi: 10.1117/12.2063489

Tokovinin, A. 2016,, 1 Zenodo, doi: 10.5281/zenodo.61119

Tokovinin, A. 2018, ApJS, 235, 6, doi: 10.3847/1538-4365/aaa1a5

Tokovinin, A. 2022, AJ, 163, 161, doi: 10.3847/1538-3881/ac5330

Tokovinin, A. 2023a, AJ, 165, 180, doi: 10.3847/1538-3881/acc464

Tokovinin, A. 2023b, AJ, 165, 220, doi: 10.3847/1538-3881/acca19

Tokovinin, A., Fischer, D. A., Bonati, M., et al. 2013, PASP, 125, 1336, doi: 10.1086/674012

Tokovinin, A., & Latham, D. W. 2017, ApJ, 838, 54, doi: 10.3847/1538-4357/aa6331

Tokovinin, A., Mason, B. D., Hartkopf, W. I., Mendez, R. A., & Horch, E. P. 2015, AJ, 150, 50, doi: 10.1088/0004-6256/150/2/50

Tokovinin, A., Mason, B. D., Mendez, R. A., & Costa, E. 2022, AJ, 164, 58, doi: 10.3847/1538-3881/ac78e7

Tokovinin, A., Mason, B. D., Mendez, R. A., & Costa, E. 2024, AJ, 168, 28, doi: 10.3847/1538-3881/ad4d56

Torres, C. A. O., Quast, G. R., da Silva, L., et al. 2006, A&A, 460, 695, doi: 10.1051/0004-6361:20065602

Pecaut, M. J., & Mamajek, E. E. 2013, ApJS, 208, 9, doi: 10.1088/0067-0049/208/1/9

[5] http://vizier.u-strasbg.fr/viz-bin/VizieR-4?-source=J/ApJS/235/6 and https://www.ctio.noirlab.edu/~atokovin/stars/